Photonics Based on Nano-Silicon

M. Ivanda[1], U. V. Desnica[1], P. Biljanović[2], K. Furić[1] and H. Gebavi[1]

[1]Ruđer Bošković Institute, P.O. Box 180, 10002 Zagreb, E-Mail: ivanda@rudjer.irb.hr
[2]Faculty for Electrotechnic and Computing, University of Zagreb, Unska 3, 10000 Zagreb

Abstract - Speed and complexity of integrated circuits are more and more increasing as integrated technology advances. The possible replacement of electrical with optical interconnects has promising potentialities in high speed performance. Optical interconnects become more and more essential and, therefore, microphotonic attempts to combine photonic and electronic components on a single Si chip. Nanosized low dimensional silicon shows photon confinement and photon trapping with evidences of light localization and light emission. In addition, many claims to have a silicon based laser within a short period have appeared in the literature by many of the researchers involved in this field. Throughout this presentation describes the research carried out at Ruđer Bošković Institute on the studies on optical gain in silicon nanocrystals to realize a Si laser. Ion implantation was used to synthesize two specimens of silica layer containing Si nanocrystals in fused quartz with different average sizes. The optical properties are studied with emphasis on optical waveguiding (WG) of the photoluminescence (PL). The WG layers were estimated to be 0.6 µm thick. We observed efficient (long-distance) propagation of the PL light in the layers. Efficient narrowing of the PL spectrum (down to 12 meV) was detected demonstrating spectral filtering by the waveguide. By using variable strip length method the optical gain spectra were measured at room temperature using cw laser excitations at different wavelengths.

I. INTRODUCTION

In spite of high efficiency emitter devices can be obtained from III-V semiconductor compounds; its integration in the current silicon (Si) planar technology is very complex and often ineffective. On the other hand silicon is a very poor emitter due to its indirect band gap. However, in nanocrystal form (Si-nano), silicon properties change drastically presenting a direct band gap with emission in the wavelength range of [600-1000] nm [1], depending on the nanocrystal size distribution.

Numerous methods have been developed to form silicon nanocrystals, and the optical properties of these materials have attracted considerable research interest. Overcoming of the electronic interconnection bottleneck is one of the main motivation and opportunity for the present-day Si-based microphotonic [2]. Replacement of some of electrical with optical interconnects has appealing potentialities, such as high speed performance. Microphotonic attempts to combine photonic and electronic components on a single Si chip. This possibility of full integration could lead to the almost unlimited performances of the highly developed silicon technology. The recent research resulted on the optoelectronic application of the silicon can be summarized as follows:

a) Porous Si Sensors

The sponge structure of PS is the cause of the high surface/volume ratio ,which is typically of the order of 500 m^2/cm^3. This is responsible for the high reactivity of PS layers in contact with chemical species. This feature is an advantage if PS is exploited as a sensing material [3]. The sensing activity of PS ranges from NO_2 [4], to humidity [5], to organic molecules like ethanol [6], etc. In addition, PS microcavities have been used as biosensor because of their response to DNA molecules and lipids [7], which allows distinguishing viral genetic chains and gram-negative bacteria. Therefore the fields of application of PS sensors are very assorted.

b) Macroporous Si as a photonic crystal

The rational behind the use of photonic crystals (PC) in optoelectronic devices can be found elsewhere [8]. Si is a good candidate to develop two-dimensional 2D photonic crystals in Si by anodic electrochemical dissolution. Electrochemical dissolution process has many advantages with respect to other dry methods: it is simpler, cheaper, faster, technologically friendly and wafer scalable.

c) Optical gain in Si-nc

Photonic properties of Si can be improved by optical doping, i.e. by introduction of efficient radiative recombination centers. Erbium has become the optical dopant of choice, in view of the fact that its emission wavelength of ~1500 nm is suitable for telecommunication applications. Optical gain comparable to that obtained in direct-gap semiconductors has been reported in ion-implanted specimens [9-12]. Er-implanted silicon nanocrystal composites have recently been embedded within distributed Bragg reflectors to produce highly directional and spectrally narrow emission [13,14], and electroluminescent device structures. Moreover, it has been recently discovered [PRL 90 (2003)] preferential production

of a single type of an optically active Er-related center in crystalline silicon. This high concentration of a specific center (labeled Er-1) was found in Er-doped Si nanolayers grown by sublimation MBE and annealed under the appropriate conditions. In that way a major breakthrough on the way toward silicon photonics based on Er doping has been achieved. It has been established that spectral characteristics of emission related to the Er-1 center will allow for two order of magnitude increase of the expected gain coefficient, when compared to the implanted Si:Er materials used so far. Therefore the Er-1 center emerges as a plausible candidate for achieving population inversion and stimulated emission in Si based materials: a long sought after goal of semiconductor science and technology.

On the other side, in visible spectral range, the recent discovery of the optical gain in silicon nanocrystals embedded in SiO_2 matrix promises soon fabrication of silicon laser [9]. The light amplification was proved using the picosecond light pumping pulses in variable strip method and by measuring the gain by pump and probe technique.

However, although various approaches to silicon photonics (quantum confinement in nanostructures and in homogeneous Si-based media, optical doping), are being actively explored, lasing action, or even intense room-temperature emission from (crystalline) silicon structures still needs to be convincingly demonstrated.

In this paper we provide further evidences for the optical gain in nanocrystaline silicon formed by high-dose ion beam synthesis in fused silica matrix. These samples exhibit intense PL and dose dependent optical absorption. By using variable strip method we show experimentally that a layer of silicon nanocrystals, prepared by the Si-ion implantation into a synthetic silica slab and exhibiting room-temperature red photoluminescence, can serve simultaneously as a single-mode planar optical waveguide. The waveguide is shown to self-select guided longitudinal and transverse electric modes from the broad photoluminescence emission of the nanocrystals resulting in a substantially narrower emission spectrum for these modes.

II. EXPERIMENT

Silicon nanoclusters were formed by multiple energy implantation of Si at around 400 keV into fused silica glass matrices ~1 mm thick Corning 7940 followed by 1 h of annealing at 1100 °C in flowing Ar 4% H2. Under these implantation and annealing conditions, the peak excess Si concentration is ~2 x $10^{22}/cm^3$ and nanocrystals with diameters of ~5.5 nm are formed in the SiO_2 matrix (sample S1). Si nanocrystals are nearly spherical and are randomly oriented relative to one another. Nanocrystal size can be decreased by reducing the dose, the annealing temperature, or the annealing time. If the concentration is reduced to $5x10^{21}/cm^3$, the Si nanocrystals are 3.5 nm diameter (Sample S2). These sizes were estimated by use of transmission electron microscope (TEM). The clusters in both samples were spherical and crystalline. The projected range of excess Si is ~600 nm and the profile has a full width at half maximum of ~300 nm. The samples were irradiated with the argon and krypton ion laser excitation lines at 514.5 and 647 nm respectively. A cylindrical lens was used to focus the laser beam on the surface on a strip of 15 and 30 μm wide for the 647 and 514.5 nm excitations, respectively and of variable length. Only the central part of the laterally focused spot was used to excite the sample ensuring the constant laser power density on the sample. Measurements show that in this case the laser power density is independent on the strip length. An objective of focal length 75 mm f/1.4 was used to focus the light from the edge of the sample onto the first slit of the spectrometer. The slit width was set to be 50 μm. The near-infrared spectra were recorded with a Spex-double monochromator equipped with a CCD detector.

III. RESULTS AND DISCUSSION

Ion implantation is a proven method to grow isolated nanoclusters of many materials in virtually any matrix. It is also widely used and effective method for forming luminescent Si nanocrystals embedded in an optically transparent matrix such as fused quartz [15]. Many authors favor a ''pure'' quantum confinement model in which the emission is due to bandgap recombination [16–20]. Accordingly, the emission energy should depend directly on nanocrystal size, and recent work has proposed a direct relationship between particle size and emission wavelength [21]. However, other work is inconsistent with this model, but instead attributes the luminescence to surface traps (e.g. [22]). The broad red PL band is proposed to arise from carrier trapping and recombination at surface Si=O bonds [23,24] that produce stable states in the gap [25]. The silicon dangling bond appears to be the main nonradiative recombination site, as determined by electron spin resonance measurements [26].

Each of our samples has a pronounced absorption edge, and the absorption edge shifts to higher energies as the dose (particle size) decreases. The absorption edges shift from the value of 2.5 eV of the sample S1 to the higher energies of 3.9 eV of the sample S2 when the dose is reduced by an order of magnitude [27]. This is qualitatively consistent with quantum confinement also, but the shift in the absorption edge toward higher energies is much

greater (by a factor of 10) than the shift in peak PL intensity as the dose is reduced. Clearly, the PL arising from Si nanoparticles in SiO_2 cannot be attributed to the conventional band edge luminescence. The PL properties of Si nanocrystals encapsulated in SiO_2 are similar in many respects to those of porous Si, and it is likely that the same mechanisms are responsible for the PL from these materials. In spite of the many investigations of porous Si, the mechanisms responsible for light emission remain controversial. In some cases, PL from porous Si has been attributed to radiative recombination of quantum confined excitons in the two dimensional quantum wire structure of porous Si [28,29]. Others have suggested that the light emission in porous Si arises from surface states localized to the boundary of the crystallites [30-31]. Likewise, PL arising from Si nanocrystals produced by Si implantation has been attributed by some investigations to quantum confinement [32,17], while others [33] have concluded that surface states play an important role.

Optical gain and stimulated emission in strongly confined nanocrystaline quantum dots (NQD) intrinsically relies on multiparticle states or more specifically, on doubly excited nanoparticles quantum confined biexcitons [33,34]. In this paper we perform quantitative analysis of Si NQD optical gain properties using variable-stripe-length (VSL) measurements of amplified spontaneous emission (ASE) [35]. This analysis indicates the importance of excitons in contributions to emission intensities for quantifying optical gain magnitudes.

In the VSL method, part of the spontaneous luminescent radiation with the spontaneous emission in an appropriate emission solid angle Ω. J_{sp} propagates along the stripe axis, and is amplified in the excited region by stimulated emission. The amplified spontaneous emission intensity, $I_{A.S.E.}$, that is emitted from the sample edge is linked with the excited stripe region length l by the relation

$$I_{A.S.E.}(l) \propto \frac{J_{sp}(\Omega)}{g_N}\left[e^{g_N l} - 1\right], \qquad (1)$$

where g_N is the net modal gain coefficient, i.e. difference between gain g and the passive propagation losses α in waveguide.

On the basis of Eq. (1), by dividing the emission spectrum at stripe length $2l$, $I_{ASE}(2l)$, with the emission spectrum at length l, $I_{ASE}(l)$, it is possible to derive the relation for the spectral dependence of the net modal gain

$$g_N(E) = \frac{1}{l}\left[\ln\left(\frac{I_{ASE}(E,2l)}{I_{ASE}(E,l)} - 1\right)\right] \qquad (2)$$

Figure 1 shows a set of room-temperature emission spectra for the S1 sample recorded using a VLS

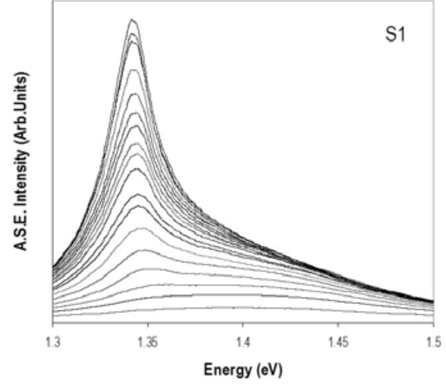

Fig. 1. Room temperature amplified spontaneous emission (A.S.E.) spectra of the sample S1 in dependence on the strip length starting with 50 μm for the low intensity spectrum with a constant increase by 50 μm up to 700 μm for the highest intensity spectrum.

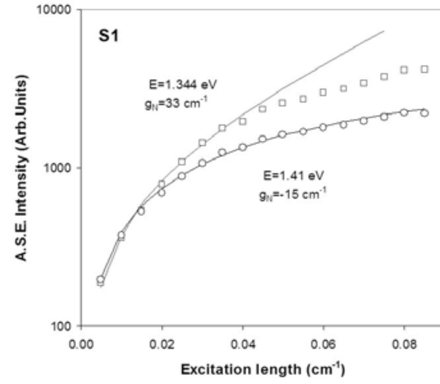

Fig. 2. ASE intensity as a function of the excitation stripe length for the sample S1 and the laser excitation energy of 1.916 eV (647 nm). The lines are fits on the data with Eq. (1) from the text. Contrary to the absorption at energy of 1.41 eV, the peak at 1.344 eV (922 nm) shows positive net modal gain of 33 cm^{-1}.

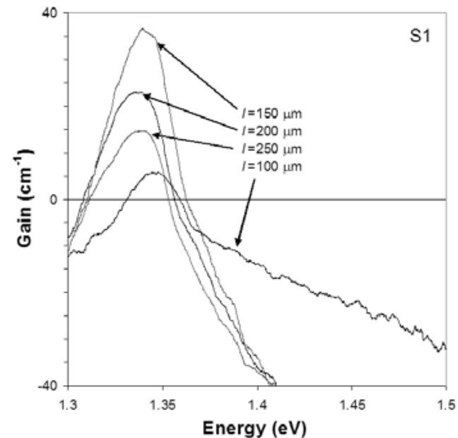

Fig. 3. Spectral dependence of the net modal gain for different stripe lengths l determined on the basis of Eq. (2).

configuration and 1.916 eV (647 nm) excitation. Development of the ASE narrow peak at 1.344 eV occurs at a threshold stripe length of 0.015 cm.

In order to take into account the existence of two types of emitters (for eample excitons and biexcitons) and the fact that optical gain in NQDs is dominated by the second mechanism, the ASE formula can be rewritten as $I_{ASE}=A_1 l + A_2 exp(g_{N2} l)/g_{N2}$, where A_1 and A_2 are constants proportional to spontaneous emission power densities for the mechanism 1 and 2, respectively, and g_{N2} is the net modal gain of the mechanism 2. Using this formula, we can simultaneously fit both below-and above-threshold regions of the I_{ASE} versus l dependence (line in Fig. 2), which yields g_{N2}=33 cm^{-1} for the peak at 1.344 eV. This estimate represents effective modal gain per unit stripe length measured for waveguide modes. To estimate the net modal gain in the absence of waveguiding effects i.e., gain per unit propagation length along the ray we can scale g_{N2} by a correction factor $\beta=n_{gl}/n_{NQD}\approx 0.88$ (n_{gl} is the index of a glass substrate), which yields $g_{N2}*\beta$ =30 cm^{-1} (this estimate assumes that the ASE is dominated by the mode that corresponds to the critical angle of the total internal reflection).

Figure 3 shows spectral dependance of the net modal gain for different excitation strip length. The positive value is observed for the spectral range 1.31-1.36 eV (of 30 meV width).

Figure 4 shows the ASE spectra taken with 2.41 eV (514.5 nm) laser excitation. The largest net modal gain g_N=90 is observed for the peak at 1.76 eV (Fig. 5). We note that the drop of the intensities for the energies below 1.45 eV is caused by the lower sensitiviy of the spectrometer detecor. The spectral dependence of the net modal gain is show on Fig.6.

Figure 7 shows the strong ASE intensity observed on the sample S2 excited with 2.41 eV laser line. The net modal gain g_N=43 is found for the ASE peak intensity at 1.59 eV (Fig. 8). The positive net modal gain here exist in a broad spectral range (Fig. 9).

The polarized measuremens were performed on the both sample by using the 2.41 nm laser. The polarized (TE) and depolarized (TM) propagating waveguide modes have been observed for the both samples (Fig.10).

The optical gain and hence possible stimulated emission in Si NQDs is dominated by quantum confined excitons and biexcitons ~single and doubly excited dots. However, because of their short lifetimes, which are limited by nonradiative Auger recombination, excitons biexcitons are not pronounced in comparison of efficiencies of Auger decay.

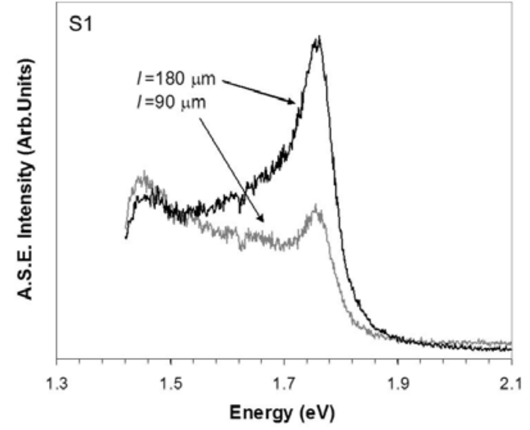

Fig. 4. Room temperature amplified spontaneous emission (A.S.E.) spectra of the sample S1 for two strip excitation length.

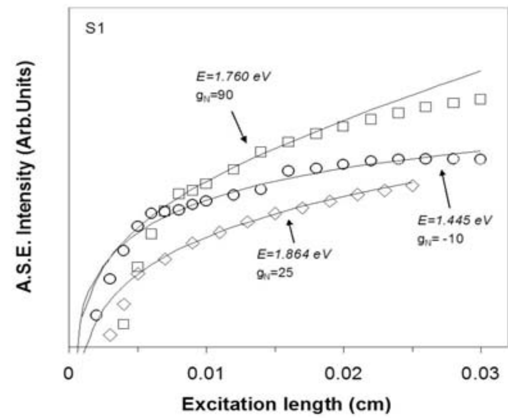

Fig. 5. ASE intensity as a function of the excitation stripe length for the sample S1 and the laser excitation energy of 2.41 eV (514.5 nm). The lines are fits on the data by Eq. (1) from the text.

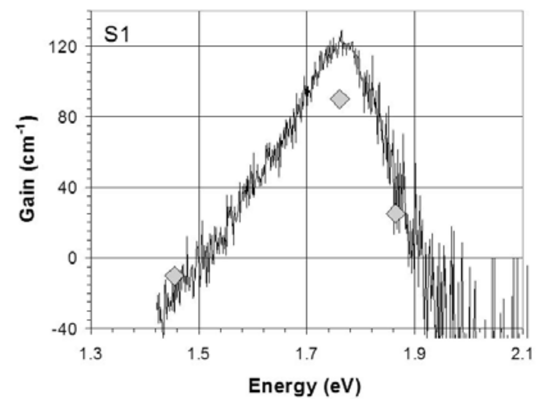

Fig. 6. Spectral dependence of the net modal gain for the excitation stripe lengths l=100 μm. The diamonds are the values from the previous figure.

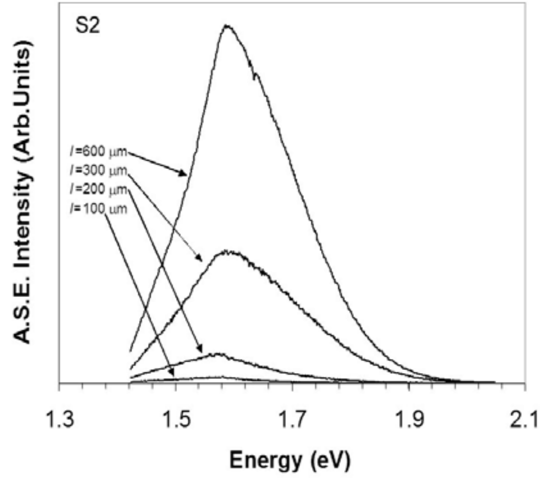

Fig. 7. Room temperature amplified spontaneous emission (A.S.E.) spectra of the sample S2 for different strip excitation lengths.

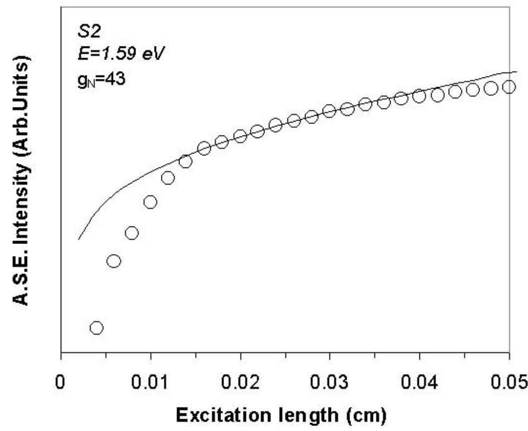

Fig. 8. ASE intensity as a function of the excitation stripe length for the sample S2 and laser excitation energy of 2.41 eV. The line is a fit by Eq. (1).

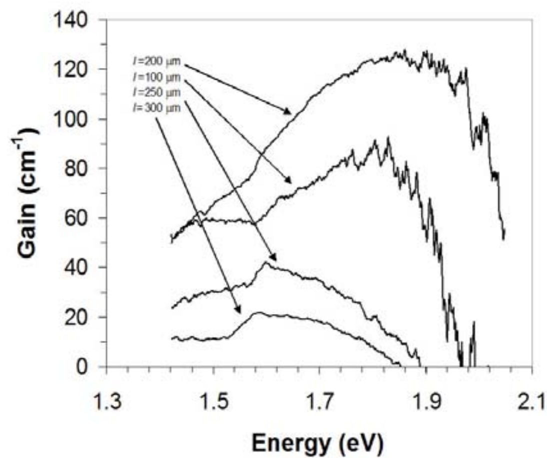

Fig. 9. Spectral dependence of the net modal gain for different excitation stripe lengths l=100 μm.

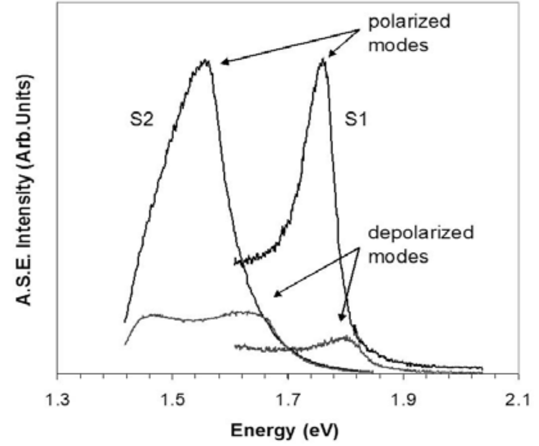

Fig. 10 Polarized (TE) and depolarized (TM) waveguide modes excited with 2.41 eV laser excitation.

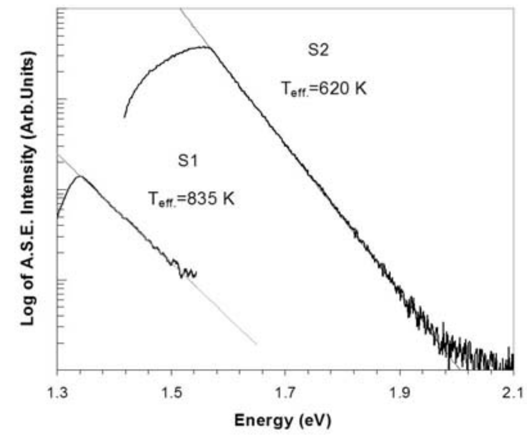

Fig. 11. Exponential tail at high-energy wing for the samples Sl and S2 with fitted values (straigt lines) for thermalized distribution of excitons.

Since in our case we excite highly above the band gap, we have to consider that the excitons thermalise, giving rise to a moderate lattice heating, also, more importantly, due to the short exciton lifetime the distribution of localized excitons is described by an effective exciton temperature T_{eff}>T(lattice temperature). In Figure 11 it is evident that each spectrum exhibits exponential tail at high-energy wing which is typical for thermalised distribution of excitons. This could be related to the emission from the band-edge excitons in silicon nano-particles, or in SiO_x interface layer. The distribution of excitons is described by the statistics ~ $\exp(-E/kT_{eff})$ of Boltzmann, where T_{eff} is the effective temperature of the excitons. The effective temperature can be found from fitting the high-energy wing of the ASE spectra as shown on Fig.11. In this way we obtain Teff~835 K for the sample S1 and Teff~620 K for the sample S2.

IV. CONCLUSION

Gain has been measured by the variable strip length method where the amplified spontaneous emission intensity, which is emitted from the sample edge, is measured as a function of the excitation volume. Exponential increase, line narrowing and directionality of stimulated emission have been measured. Material gain values as high as those typically found in III-V semiconductors quantum dots have been measured.

To have a Si laser, or in general, a laser, one needs three key ingredients: i) an active material, which should be luminescent in the region of interest and able to amplify light, ii) an optical cavity, iii) a suitable and efficient pumping scheme to achieve and sustain the laser action. If this objective is realized all the major building blocks for monolithic silicon microphotonics will be available. The final vision is to have Si microphotonics participating in every global application of the photonics industry: computing, communications, imaging, medicine, optical sensing of physical, chemical and biological inputs, optical storage, etc.

ACKNOWLEDGMENTS

This work was supported by the Ministry of Science and Technology of the Republic of Croatia under contracts TP-01/0098-23 and 00980303.

REFERENCES

[1] L.T. Canham, Appl. Phys. Lett. **57** (1990) 1046.
[2] T. Shimizu-Iwayama, T. Hama, D.E. Hole, I.W. Boyd, Solid State Electron. **45** (2001) 1487.
[3] V. Mulloni and L. Pavesi, Appl. Phys. Lett. **76** 2523, (2000).
[4] C. Baratto, G. Faglia, G. Sberveglieri, L. Boarino, A. M. Rossi and G. Amato, Thin Solid Films **391,** 261 (2001).
[5] A. Foucaran, B. Sorli, M. Garcia, F. Pascal-Delannoy, A. Giani and A. Boyer, Sens. Act. A **79,** 189 (2000).
[6] Z. Gaburro, N. Daldosso, L. Pavesi, G. Faglia, C. Baratto and G. Sberveglieri, Appl. Phys. Lett. **78** 3744 (2001).
[7] S. Chan, P. M. Fauchet, Y. Li, L. J. Rothberg and B. L. Miller, Phys. Stat. Sol. A **182,** 541 (2000).
[8] C. Weisbuch, H. Benisty, S. Olivier, M. Rattier, C. J. M. Smith and T. F. Krauss. Phys. Stat. Sol. (b) **221,** 93 (2000).
[9] L. Pavesi, L. Dal Negro, C. Mazzoleni, G. Franzo and F. Priolo, Nature (London) **408,** 440 (2000).
[10] M. Ivanda, U.V. Desnica, C. W. White and W. Kiefer, NATO Science Series Vol. **93**: Towards the First Silicon Laser, pp. 191-196, L. Pavesi, S. Gaponenko and L. Del-Negro (eds.), Kluwer Academic Publishers, Netherlands, 2003.
[11] G. Franz_o, V. Vinciguerra, F. Priolo, Appl. Phys. A **69**, 436 (1999).
[12] M. Fujii, M. Yoshida, Y. Kanzawa, S. Hayashi, K.Yamamoto, Appl. Phys. Lett. **71** (1997) 1198.
[13] F. Iacona, G. Franz_o, E.C. Moreira, D. Pacifici, A. Irrera, F. Priolo, Mater. Sci. Eng. C **19** (2002) 377.
[14] S. Chan, P.M. Fauchet, Opt. Mater. **17** (2001) 31.
[15] T. Shimizu-Iwayama, T. Hama, D.E. Hole, I.W. Boyd, Solid State Electron. **45** (2001) 1487.
[16] E. Neufeld, S. Wang, R. Apetz, Ch. Buchal, R. Carius, C. W. White, D. K. Thomas, Thin Solid Films **294** (1997) 238.
[17] P. Mutti, G. Ghislotti, S. Bertoni, L. Bonoldi, G. F. Cerofolini, L. Meda, E. Grilli, M. Guzzi, Appl. Phys. Lett. **66** (1995) 851.
[18] M.L. Brongersma, P.G. Kik, A. Polman, K. S. Min, H.A. Atwater, Appl. Phys. Lett. **76** (2000) 351.
[19] V. Vinciguerra, G. Franz_o, F. Priolo, F. Iacona, C. Spinella, J. Appl. Phys. **87** (2000) 8165.
[20] J. Valenta, J. Dian, K. Luterova, P. Knapek, I. Pelant, M. Nikl, D. Muller, J. J. Grob, J. L. Rehspringer, B. Honerlage, Eur. Phys. J. D **8** (2000) 395.
[21] C. Garcia, B. Garrido, P. Pellegrino, R. Ferre, J. A. Moreno, J.R. Morante, L. Pavesi, M. Cazzanelli, Appl. Phys. Lett. **82** (2003) 1595.
[22] K. S. Zhuralev, A. M. Gilinsky, A. Y. Kobitsky, Appl. Phys. Lett. **73** (1998) 2962.
[23] G. Allan, C. Delerue, M. Lannoo, Phys. Rev. Lett. **76** (1996) 2961.
[24] I. Vasiliev, J. R. Chelikowski, R. M. Martin, Phys. Rev. B **65** (2002) 121302.
[25] D. Kovalev, J. Diener, H. Heckler, G. Polisski, N. Keunzner, F. Koch, Phys. Rev. B **61** (2000) 4485.
[26] M. Lopez, B. Garrido, C. Garcia, P. Pellegrino, A. Perez- Rodriguez, J. R. Morante, C. Bonafos, M. Carrada, A. Claverie, Appl. Phys. Lett. **80** (2002) 1637.
[27] C.W. White J.D. Budai, S.P. Withrow, J.G. Zhu, E. Sonder, R.A. Zuhr, A. Meldrum, D.M. Hembree, Jr., D.O. Henderson, S. Prawer, Nucl. Instr. and Meth. in Phys. Res. B **141** (1998) 228.
[28] R. T. Collins, P. M. Fauchet, and M. A. Tischler, Physics Today, January 1997, p. 25.
[29] F. Koch, V. Petrova-Koch, T. Muschik, A. Nikolov, V. Gavrilenko, Mat. Res. Soc. Symp. Proc. 283 (1993) 197; F. Koch, V. Petrova-Koch, T. Muschik, J. Lumin. **57** (1993) 271.
[30] Y. Kanemitsu, H. Uto, Y. Masumoto, T. Matsu-moto, T. Futagi, H. Mimura, Phys. Rev. B **48** (1993) 2827.
[31] S.M. Prokes, J. Mat. Res. **11** (1996) 305.
[32] K. S. Min, K. V. Shcheglov, C. M. Tang, H. A. Atwater, M.L. Brongersma, A. Polman, Appl. Phys. Lett. **69** (1996) 2033.
[33] V. I. Klimov, A. A. Mikhailovsky, S. Xu, A. Mal-ko, J. A. Hollingsworth, C. A. Leatherdale, H.-J. Eisler, and M. G. Bawendi, Science **290**, 314 (2000).
[34] A. A. Mikhailovsky, A. V. Malko, J. A. Hollings-worth, M. G. Bawendi and V. I. Klimov, Appl. Phys. Lett. **80**, 2380 (2002).
[35] K. L. Shaklee, R. E. Nahory, and R. F. Leheny, J. Lumin. 7, 284, (1973).